PAPER • OPEN ACCESS

Role of sea surface warming in convective activity over Europe and Northern Eurasia: estimates with sensitivity model experiments

Role of sea surface warming in convective activity over Europe and Northern Eurasia: estimates with sensitivity model experiments

Yu I Yarinich[1,2], A V Chernokulsky[1], V A Semenov[1,3], M Latif[4]

[1] A.M. Obukhov Institute of Atmospheric Physics, Russian Academy of Sciences, Pyzhevsky 3, Moscow, 119017, Russia

[2] Lomonosov Moscow State University, Leninskie Gory 1, Moscow, 119991, Russia

[3] Institute of Geography, Russian Academy of Sciences, Staromonetny 29, Moscow, 119017, Russia

[4] GEOMAR Helmholtz Centre for Ocean Research Kiel, 24105 Kiel, Germany

E-mail: a.chernokulsky@ifaran.ru

Abstract. The influence of sea surface warming on convective activity over Europe and Northern Eurasia is estimated from sensitivity model experiments by an atmospheric general circulation model, ECHAM5, with prescribed boundary conditions ("warm" and "cold" sea surface). Convective activity is analysed by using various indices (thermodynamic, dynamic, and composite). It is shown that warmer sea surface leads to a general increase in the thermodynamic indices that is broadly consistent with observations. Particularly, the observed increase in CAPE over the eastern part of the Mediterranean Sea, the Black Sea, and Eastern Europe is well reproduced in the sensitivity experiments. At the same time, the shear and helicity instability indices depend little on sea surface warming. The experiment with only Mediterranean and Black Seas warming tends to overestimate the increase in the thermodynamic indices near these seas and underestimate the increase in the other regions. There are several regions (the Iberian Peninsula, Mongolia, and Northern China) where the observations show a decrease in the convective indices. These negative changes are not reproduced in the model experiments, because their nature is, apparently, not related to sea surface warming.

1. Introduction

The convective processes over Europe and Northern Eurasia become more prominent, which is manifested in an increase of the convective cloudiness [1-4], convective precipitation [5-8], the occurrence of thunderstorms [9], and severe convection environments [10-12]. In particular, Figure 1 shows the difference in CAPE (convective available potential energy) between 2000–2012 and 1979–1999 in the summer season based on ERA-Interim data [13]. With some regional exceptions, both the mean and frequency of exceeding the threshold tend to increase in the second period.

These changes may depend on different factors including thermodynamics (e.g., increase in the surface temperature and humidity, changes in the lapse rate [14,15]), dynamics (e.g., changes in cyclones and activity of atmospheric fronts [16-18], moisture convergence [19,20]), and microphysics (e.g., influence of aerosols [21]). In turn, both local and global warming and moistening of the lower

atmosphere can be important. In particular, an important role of warm seas (the Mediterranean, Black, and Caspian seas) in the formation of strong tornadoes [22-24] and heavy convective precipitation events [25, 26] over Europe and Northern Eurasia was highlighted. It should be noted that the largest increase of the CAPE (Fig.1) is observed above the Eastern Mediterranean, Black, and Caspian Seas. The role of different factors in changes of the convective activity in the Eurasian midlatitudes should be quantitatively estimated for increasing our ability to predict severe convective events and project their changes in the 21st century.
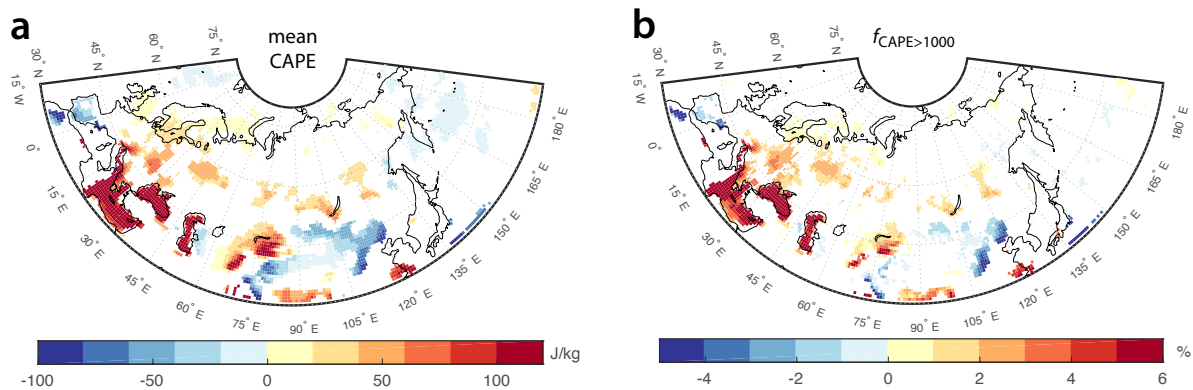
Figure 1. Difference between 2000–2012 and 1979–1999 of (a) summer-mean CAPE and (b) frequency of CAPE>1000 J kg^{-1} in summer based on ERA-Interim reanalysis data. Only significant changes are shown (see the definition of *significant changes* in Section 2).

One of the approaches to discriminate the role of different factors is to analyze specially designed sensitivity model experiments [25-27]. Particularly, Meredith and co-authors [25] used model simulations with warm and cold SST and highlighted the enhancement of local lower tropospheric instability due to the current warmer Black Sea. This enhancement triggers deep convection and increases precipitation by more than 300% between warm and cold SSTs during single events, as in July 2012 near the town of Krymsk [25]. A similar approach was used to estimate the influence of Mediterranean Sea warming on extreme precipitation formation in Europe [26].

In this study, the impact of sea-surface warming (global ocean warming and the Mediterranean and Black Seas only warming) on the convective activity changes over Northern Eurasia and Europe is estimated based on sensitivity experiments with the atmospheric general circulation model (AGCM). Convective activity in the atmosphere is estimated based on analysis of various convective indices. The approach for analysis of convective indices using the results of global climate model simulation was used previously for the USA [28,29], Australia [30,31], and Europe [32].

2. Data and method
We analyzed three numerical experiments with the AGCM ECHAM5 that are identical except for sea-surface temperature (SST) and sea ice concentration (SIC). The control experiment was forced globally with monthly climatological fields of 1970–1999 SST and SIC [26] (so-called 'cold ocean experiment', CO). In the warm Mediterranean experiment (WM), the warmer 2000–2012 SST climatology was employed only in the Mediterranean and Black Seas. In the global warm experiment ('warm ocean', WO), the ECHAM5 was forced globally with monthly climatological fields of 2000–2012 SST and SIC. For each experiment, a 40-member ensemble of one year was computed. The model was integrated at a relatively high horizontal resolution for a global atmosphere model of T159 (approximately 75 km) and with 31 vertical levels. Forcing conditions for all experiments were taken from the Hadley Centre Sea Ice and Sea Surface Temperature dataset [33]. Radiative and greenhouse gas forcing was fixed to the present-day levels [26].

Based on 6-hour model data, various convective instability indices were calculated including thermodynamic (CAPE, CIN) [34-36] and dynamic indices (SRH, DLS) [37,38], as well as composite parameters (WMAXSHEAR, EHI) [35,39] and a simplified index 3D [40,41] (Table 1).

Table 1. Analysed convective indices.

Index (acronym)	Index (full name)	Formula	Threshold
CAPE*, J Kg^{-1}	Convective available potential energy	$\text{CAPE} = \int_{LFC}^{EL} g\left(\dfrac{T_{v,parcel} - T_{v,env}}{T_{v,env}}\right) dz$	0, 100, 1000, 2500
CIN*, J Kg^{-1}	Convective inhibition	$\text{CIN} = \int_{surf}^{LFC} g\left(\dfrac{T_{v,parcel} - T_{v,env}}{T_{v,env}}\right) dz$	10, 30, 50
SRH, m^2 s^{-2}	Storm relative helicity	$\text{SRH} = \int_{surf}^{3km} \left(\vec{v}_{hor} - \vec{c}\right)\vec{\omega}_{hor}\, dz$	160, 300, 400
DLS, m s^{-1}	Deep layer shear	$\text{DLS} = \Delta V_{500-950}$	20, 30, 40
WMAXSHEAR, m^2 s^{-2}	WMAXSHEAR	$\text{WMAXSHEAR} = \text{DLS} \times (2\text{CAPE})^{-1/2}$	300, 450, 600
EHI	Energy-helicity index	$\text{EHI} = \text{CAPE} \times \text{SRH} / 160\,000$	1, 2, 3
3D, ºC	Dewpoint, depression of dewpoint index	$\text{3D} = D_{surf} - DD_{surf}$	15.5, 17, 19

The following notation is used: LFC – height of level of free convection, EL – height of equilibrium level, $T_{v,parcel}$ – virtual temperature of a specific parcel, $T_{v,env}$ – virtual temperature of the environment, D – dew point temperature, DD – depression of dew point temperature, V – wind speed. Subscripts denote vertical levels (surf – near surface; 950 and 500 – height of corresponding geopotential height).
    * Mean-level (ML) (1 km) and most-unstable (MU) CAPE and CIN were calculated.

We estimated the difference in the index values (mean, maximum, frequency of exceeding thresholds) between a pair of experiments (WO–CO, WM–CO, WO–WM) calculated for 40 modeled summer months (June, July, August). The significance of the difference was estimated based on the non-parametric Mann-Whitney U-test (the difference was called *significant* for p-values ≤0.05) [42]. In addition to the experiments with the ECHAM5 model, data from ERA-Interim reanalysis (for 1979–2012) were used as well.

3. Results
The warmer Global Ocean favors warmer and more humid near-surface air, which results in a significant increase of the CAPE (ML and MU), WMAXSHEAR, and 3D indices (both the means and frequencies of exceeding the threshold (Figures 2–4)). Exceeding of higher thresholds (e.g., 2500J kg^{-1} for CAPE and 600 m^2 s^{-2} for WMAXSHEAR) also occurs much more often in the WO experiment (not shown).

    The increase in the thermodynamic convective indices is especially pronounced over marginal seas of the Atlantic and Pacific Oceans (the Mediterranean, Black, Baltic, Japan, and Okhotsk Seas), which broadly corresponds to the observed changes of CAPE (Figure 1). The greatest increase of CAPE is found in the Black Sea and Eastern Mediterranean in both the reanalysis and sensitivity model simulations. The observed increase of CAPE over Europe (Figure 1) can be attributed to the influence of sea surface warming. Specifically, both the ML CAPE and MU CAPE (their means and frequencies of exceeding the threshold) are significantly larger in this region in the WO experiment compared to the CO. On the contrary, no positive statistically significant difference of the CAPE between the WO and CO over eastern China is revealed in the observations. No negative WO–CO difference of the CAPE and 3D was found, which is in contrast to the reanalysis data that show a decrease of the CAPE over the Iberian Peninsula, Mongolia, and Northern China (Figure1).
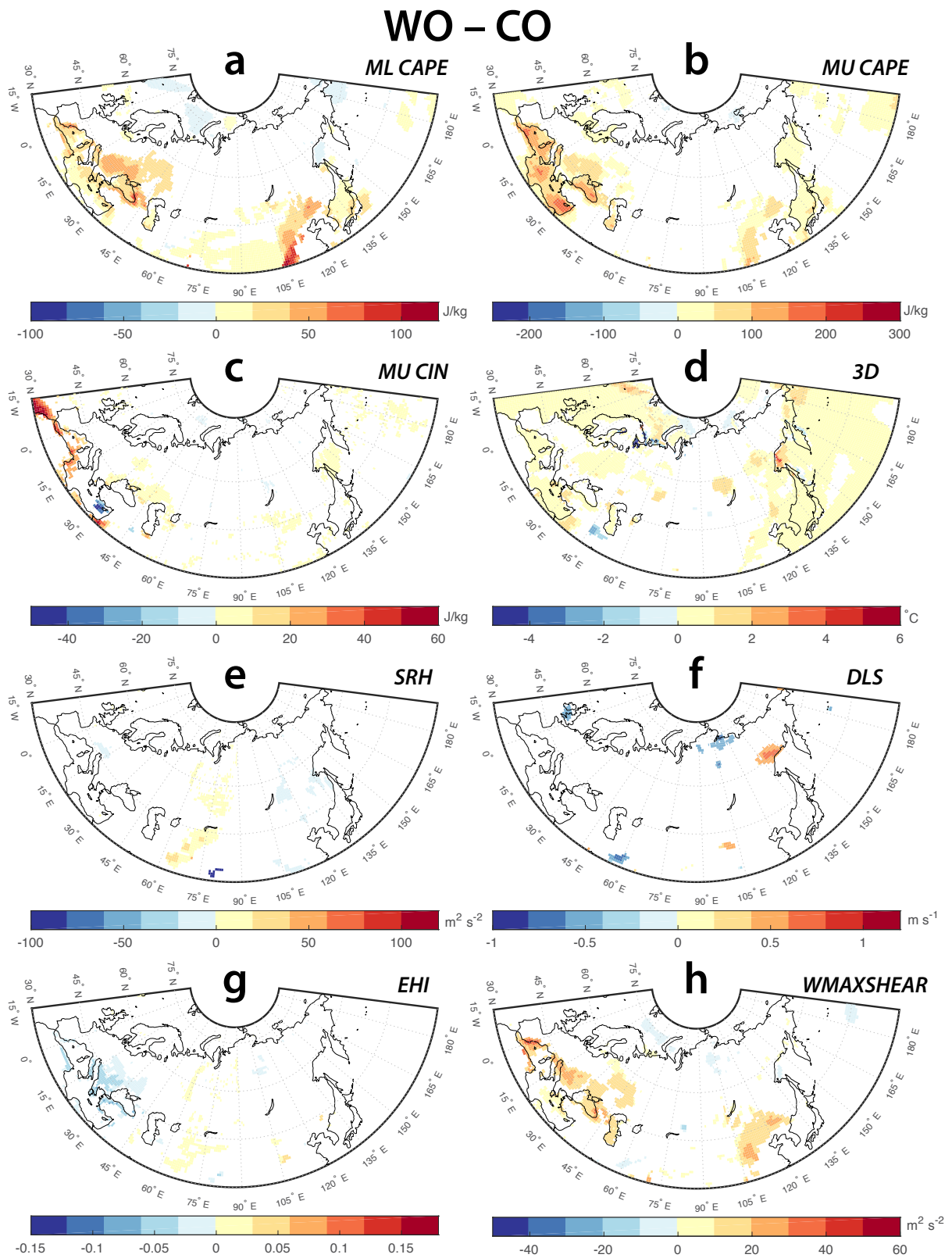
Figure 2. Difference between WO and CO for summer means of various indices: (a) ML CAPE, (b) MU CAPE, (c) MU CIN, (d) 3D, (e) SRH, (f) DLS, (g) ML EHI, (h) ML WMAXSHEAR. Only significant difference is shown.
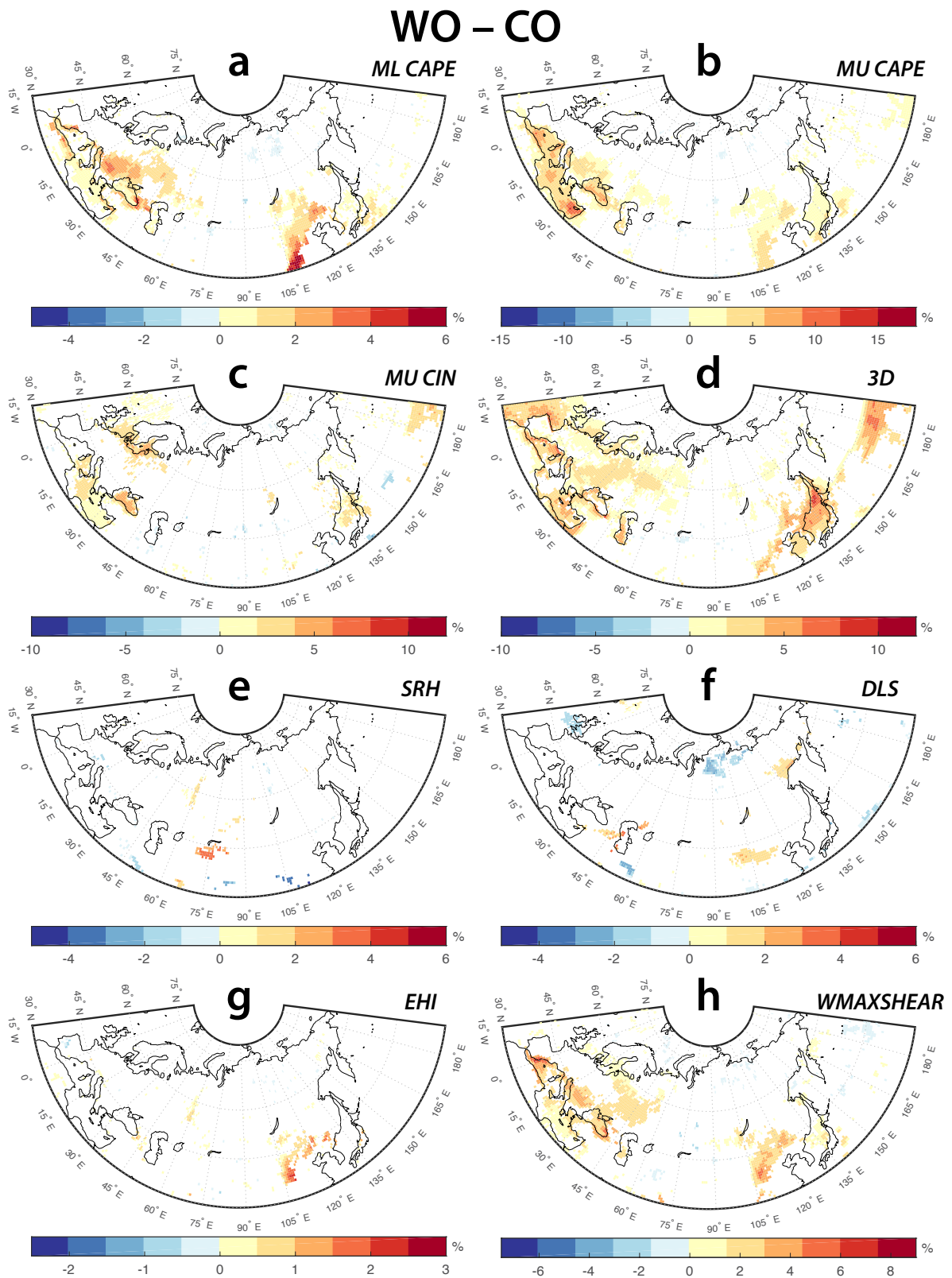
Figure 3. Difference between WO and CO for the frequency of exceeding the threshold in summer for different indices: (a) ML CAPE>1000 J kg^{-1}, (b) MU CAPE > 1000 J kg^{-1}, (c) MU CIN < 30 J kg^{-1}, (d) 3D > 15.5 ºC, (e) SRH > 160 m^2 s^{-2}, (f) DLS > 20 m s^{-1}, (g) ML EHI > 1, (h) ML WMAXSHEAR > 300 m^2 s^{-2}. Only significant changes are shown.
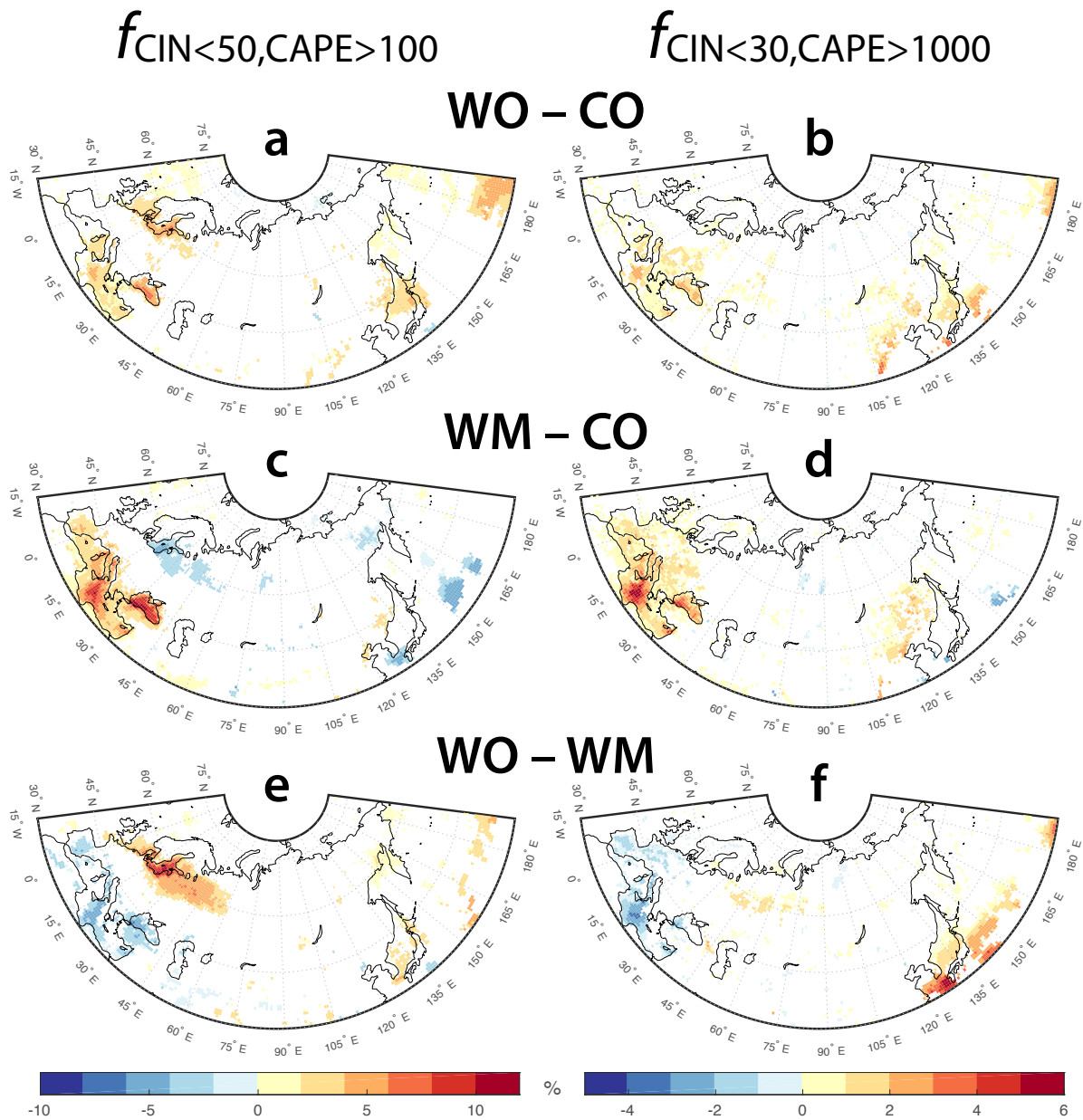
Figure 4. Differences between WO and CO (a, b), WM and CO (c, d), WO and WM (e, f) for the frequency of exceeding the threshold in summer for different indices: (a, c, e) MU CAPE>100 J kg^{-1} and MU CIN < 50 J kg^{-1}, (b, d, f) MU CAPE>1000 J kg^{-1} and MU CIN < 30 J kg^{-1}. Only significant changes are shown.

The wind shear and helicity indices (their summer means and frequencies of exceeding the threshold) do not exhibit significant changes between the CO to the WO (Figures 2 and 3).

Sea surface warming results in changes in convective inhibition. Large values of CIN (i.e., more than 100 J kg^{-1}) prevent the development of convection. Although the mean CIN is generally larger in the WO than in the CO (except for the eastern part of the Mediterranean Sea) (Figure 2), the frequency of a very low CIN is also larger in the WO (Figure 3). If these low-CIN environments co-occur with a high-CAPE, this likely initiates a severe storm [28]. The frequency of such environments is

significantly larger in the WO experiment as compared to the CO (Fig. 4a, b) in many regions (primarily over the marginal seas of the Atlantic and Pacific Oceans and Eastern Europe).

Only the Mediterranean and Black Sea surface warming (the WM experiment) results in a larger (as compared to the WO) increase of such indices as CAPE, 3D, and WMAXSHEAR (their means and frequency of exceeding the threshold) and the frequency of low-CIN/high-CAPE environments in these regions, and a lower increase (or even decrease) in other regions (Figures 4c-f).

4. Conclusions

In this paper, sensitivity experiments were performed to estimate the role of sea surface warming in convective activity over Europe and Northern Eurasia. The convective instability indices were calculated with 6-hour data from three model experiments with different boundary conditions (warm global ocean, cold global ocean, and cold ocean – warm Mediterranean and Black Seas).

A comparison of the results of the sensitivity experiments has shown that warmer sea surface leads to a general increase in the thermodynamic convective instability indices. This increase is broadly consistent with observations. Particularly, the sensitivity experiments reproduce well the observed increase in CAPE over the eastern part of the Mediterranean Sea, the Black Sea, and Eastern Europe. The 3D and WMAXSHEAR indices grow as well in the WO experiment compared to the CO. The shear and helicity instability indices depend little on sea surface warming. The WM experiment shows a greater (compared to the WO) increase in the thermodynamic indices in these very regions and a smaller increase (or even decrease) in the indices in the other regions. In particular, the observed increase in CAPE in Eastern Europe cannot be explained by the warming of the Mediterranean and Black Seas alone. Note that the above-presented results are preliminary, and further analysis is required.

The reanalysis data show a decrease in the convective indices in several regions (the Iberian Peninsula, Mongolia, and Northern China). These negative changes are not reproduced in the model experiments, because their nature is, apparently, not related to sea surface warming. For instance, a decrease in the lapse rate may prevail here over an increase in the surface temperature. Further research is needed to establish the causes of these changes. For instance, sensitivity experiments with interactive greenhouse gases should be carried out to clarify the role of lapse rate changes in the convective activity variability. Given the scale of convective phenomena, it is desirable to use regional climate models [43] or dynamic downscaling of the AGCM [44].

References

[1]   Sun B, Groisman P Y and Mokhov I I 2001 Recent Changes in Cloud-Type Frequency and Inferred Increases in Convection over the United States and the Former USSR *Journal of Climate* **14** 1864–80

[2]   Chernokulsky A V, Bulygina O N and Mokhov I I 2011 Recent variations of cloudiness over Russia from surface daytime observations **6** 035202

[3]   Chernokulsky A V, Esau I, Bulygina O N, Davy R, Mokhov I I, Outten S and Semenov V A 2017 Climatology and Interannual Variability of Cloudiness in the Atlantic Arctic from Surface Observations since the Late Nineteenth Century *Journal of Climate* **30** 2103–20

[4]   Chernokulsky A and Esau I 2019 Cloud cover and cloud types in the Eurasian Arctic in 1936–2012 *Int. J. Climatol.* **16** 14343–20

[5]   Rulfová Z and Kyselý J 2014 Trends of Convective and Stratiform Precipitation in the Czech Republic, 1982–2010 *Adv. Meteorol.* **2014** 1–11

[6]   Han X, Xue H, Zhao C and Lu D 2016 The roles of convective and stratiform precipitation in the observed precipitation trends in Northwest China during 1961–2000 *Atmospheric Research* **169** 139–46

[7]   Ye H, Fetzer E J, Wong S and Lambrigtsen B H 2017 Rapid decadal convective precipitation increase over Eurasia during the last three decades of the 20th century *Science Advances* **3** e1600944

[8]   Chernokulsky A, Kozlov F, Zolina O, Bulygina O, Mokhov I I and Semenov V A 2019 Observed changes in convective and stratiform precipitation in Northern Eurasia over the last five decades *Environmental Research Letters* **14** 045001–17

[9]   Taszarek M, Allen J, Púčik T, Groenemeijer P, Czernecki B, Kolendowicz L, Lagouvardos K, Kotroni V and Schulz W 2019 A Climatology of Thunderstorms across Europe from a Synthesis of Multiple Data Sources *Journal of Climate* **32** 1813–37

[10]   Riemann-Campe K, Fraedrich K and Lunkeit F 2009 Global climatology of convective available potential energy (CAPE) and convective inhibition (CIN) in ERA-40 reanalysis *Atmospheric Research* **93** 534–45

[11]   Chernokulsky A V, Kurgansky M V and Mokhov I I 2017 Analysis of changes in tornadogenesis conditions over Northern Eurasia based on a simple index of atmospheric convective instability *Doklady Earth Sci.* **477** 1504–9

[12]   Pistotnik G, Groenemeijer P and Sausen R 2017 Validation of Convective Parameters in MPI-ESM Decadal Hindcasts (1971–2012) against ERA-Interim Reanalyses *Meteorol. Z.* **25** 753–66

[13]   Dee D P *et al* 2011 The ERA-Interim reanalysis: configuration and performance of the data assimilation system *Quarterly Journal of the Royal Meteorological Society* **137** 553–97

[14]   Berg P, Moseley C and Haerter J O 2013 Strong increase in convective precipitation in response to higher temperatures *Nature Geosci.* **6** 181–5

[15]   Berg P and Haerter J O 2013 Atmospheric Research *Atmospheric Research* **119** 56–61

[16]   Mokhov I I, Chernokul'skii A V, Akperov M G, Dufresne J-L and Le Treut H 2009 Variations in the Characteristics of Cyclonic Activity and Cloudiness in the Atmosphere of Extratropical Latitudes of the Northern Hemisphere Based from Model Calculations Compared with the Data of the Reanalysis and Satellite Data *Doklady Earth Sci.* **424** 147–50

[17]   Berry G, Jakob C and Reeder M 2011 Recent global trends in atmospheric fronts *Geophysical Research Letters* **38** L21812

[18]   Schemm S, Sprenger M, Martius O, Wernli H and Zimmer M 2017 Increase in the number of extremely strong fronts over Europe? A study based on ERA-Interim reanalysis (1979-2014) *Geophysical Research Letters* **44** 553–61

[19]   Loriaux J M, Lenderink G and Siebesma A P 2017 Large-Scale Controls on Extreme Precipitation *Journal of Climate* **30** 955–68

[20]   Lenderink G, Barbero R and Loriaux J M 2017 Super Clausius-Clapeyron scaling of extreme hourly convective precipitation and its relation to large-scale atmospheric conditions *Journal of Climate* **30** 6037–52

[21]   Tao W-K, Chen J-P, Li Z, Wang C and Zhang C 2012 Impact of aerosols on convective clouds and precipitation *Reviews of Geophysics* **50** RG2001

[22]   Finch J and Bikos D 2012 Russian Tornado Outbreak of 9 June 1984 *E-journal of Severe Storms Meteorology* **7** 1–28

[23]   Miglietta M M, Mazon J, Motola V and Pasini A 2017 Effect of a positive Sea SurfaceTemperature anomaly on aMediterranean tornadic supercell *Sci Rep* 1–8

[24]   Shikhov A and Chernokulsky A 2018 A satellite-derived climatology of unreported tornadoes in forested regions of northeast Europe *Rem. Sens. Environ.* **204** 553–67

[25]   Meredith E P, Semenov V A, Maraun D, Park W and Chernokulsky A V 2015 Crucial role of Black Sea warming in amplifying the 2012 Krymsk precipitation extreme *Nature Geosci.* **8** 615–9

[26] Volosciuk C, Maraun D, Semenov V A, Tilinina N, Gulev S K and Latif M 2016 Rising Mediterranean Sea Surface Temperatures Amplify Extreme Summer Precipitation in Central Europe *Sci Rep* **6** 1–7

[27] Semenov V A and Latif M 2015 Nonlinear winter atmospheric circulation response to Arctic sea ice concentration anomalies for different periods during 1966–2012 **10** 1–8

[28] Diffenbaugh N S, Scherer M and Trapp R J 2013 Robust increases in severe thunderstorm environments in response to greenhouse forcing *Proceedings of the National Academy of Sciences* **110** 16361–6

[29] Seeley J T and Romps D M 2015 The Effect of Global Warming on Severe Thunderstorms in the United States *Journal of Climate* **28** 2443–58

[30] Allen J T, Karoly D J and Walsh K J 2014 Future Australian Severe Thunderstorm Environments. Part I: A Novel Evaluation and Climatology of Convective Parameters from Two Climate Models for the Late Twentieth Century *Journal of Climate* **27** 3827–47

[31] Allen J T, Karoly D J and Walsh K J 2014 Future Australian Severe Thunderstorm Environments. Part II: The Influence of a Strongly Warming Climate on Convective Environments *Journal of Climate* **27** 3848–68

[32] Marsh P T, Brooks H E and Karoly D J 2009 Atmospheric Research *Atmospheric Research* **93** 607–18

[33] Rayner N A, Parker D E, Horton E B, Folland C K, Alexander L V, Rowell D P, Kent E C and Kaplan A 2003 Global analyses of sea surface temperature, sea ice, and night marine air temperature since the late nineteenth century *Journal of Geophysical Research* **108** 14

[34] Moncrieff M W and Miller M J 1976 The dynamics and simulation of tropical cumulonimbus and squall lines *Quarterly Journal of the Royal Meteorological Society* **102** 373–94

[35] Doswell C A III and Schultz D M 2006 On the use of indices and parameters in forecasting severe storms *E-journal of Severe Storms Meteorology* **1** 1–24

[36] Kurgansky M V, Chernokulsky A V and Mokhov I I 2013 The tornado over Khanty-Mansiysk: An exception or a symptom? *Russian Meteorology and Hydrology* **38** 539–46

[37] Rasmussen E N and Blanchard D O 1998 A Baseline Climatology of Sounding-Derived Supercell and Tornado Forecast Parameters *Weather and Forecasting* **13** 1148–64

[38] Davies-Jones R, Burgess D and Foster M 1990 Test of helicity as a tornado forecast parameter. 16th Conf. on Severe Local Storms (Kananaskis Park, AB, Canada) pp 588–92

[39] Taszarek M, Brooks H E, Czernecki B, Szuster P and Fortuniak K 2018 Climatological Aspects of Convective Parameters over Europe: A Comparison of ERA-Interim and Sounding Data *Journal of Climate* **31** 4281–308

[40] Livingston R 1984 *The subsynoptic pre-tornado Environment* (Columbia: University of Missouri)

[41] Chernokulsky A V, Kurgansky M V, Zakharchenko D I and Mokhov I I 2015 Genesis environments and characteristics of the severe tornado in the South Urals on August 29, 2014 *Russian Meteorology and Hydrology* **40** 794–9

[42] Wilks D 2011 *Statistical Methods in the Atmospheric Sciences* vol 100 (Academic Press)

[43] Púčik T, Groenemeijer P, Rädler A T, Tijssen L, Nikulin G, Prein A F, van Meijgaard E, Fealy R, Jacob D and Teichmann C 2017 Future Changes in European Severe Convection Environments in a Regional Climate Model Ensemble *Journal of Climate* **30** 6771–94

[44] Gensini V A and Mote T L 2014 Estimations of Hazardous Convective Weather in the United States Using Dynamical Downscaling *Journal of Climate* **27** 6581–9